Real-time Detection of Intradialytic Hypotension using a Novel Polyvinylidene Fluoride Based Sensor

Sardar Ansari[1,*], *Member, IEEE,* Negar Farzaneh[2,*], Michael Heung[3,*], Kenn Oldham[4,*], Harm Derksen[5,*], Kevin R. Ward[6,*] and Kayvan Najarian[7,*], *Senior Member, IEEE*

***Abstract*— This paper presents a novel sensor in the form of a ring to monitor vascular tone continuously and non-invasively. The signal that is generated by this sensor would allow for accurate detection and analysis of reflection waves that can be used to identify or predict several medical conditions including intradialytic hypotension (IDH). The sensor is accompanied by signal analytics that would detect the changes in the morphology of the signal which are associated with IDH and would notify the dialysis physicians and nurses. The data that was collected from nine dialysis patients indicated that the proposed ring and the signal processing and machine learning approaches that are used can predict IDH up to one hour before the incidence of IDH.**

I. Introduction

Hemodialysis is one of the most common medical procedures in the world. For example, more than 43.5 million dialysis sessions were performed for more than 375000 patients in the US in 2013 [1]. Intradialytic hypotension (IDH) is defined as an abnormal drop in blood pressure (BP) in patients who are being dialyzed and is one of the most common complications observed during dialysis. In fact, at least one IDH episode complicates approximately 20 to 30% of dialysis sessions, making it the most common complication of this life-sustaining procedure [2], [3]. IDH has been identified as an independent risk factor for mortality, including sudden cardiac death during dialysis [4], [5]. When IDH occurs, common interventions include administering Albumin, Dextrose, IV fluids, and/or changing the ultrafiltration (UF) rate or goal. In severe cases the dialysis procedure is abruptly stopped and the patient is either rescheduled for a supplementary sitting or transported to an emergency facility for more intensive treatments. Such interventions for IDH can significantly increase the cost of a routine dialysis procedure. In 2013, cases of severe IDH reported in the United States that led to hospitalization and ER visits amounted to a total of $96M in hospital and treatment costs[6]. This does not include the large number of IDH episodes that are treated within the dialysis center. Despite several efforts to alleviate this problem, none of the existing methods have proven effective thus far. Currently, the IDH events are detected by BP measurements collected intermittently once every 5 to 15 minutes and patient reported symptoms which are highly subjective. Therefore, the present standard of care relies on reacting to IDH as it develops, rather than detecting or predicting impending IDH and trying to avert the risks associated with IDH.

A recent study has reviewed several different definitions for IDH that are used by practitioners and their association with mortality [4]. They concluded that the best criteria for defining IDH is the occurrence of systolic BP (SBP)$<$90mmHg when predialysis SBP$<$160mmHg and SBP$<$100mmHg when predialysis SBP$\geq$160mmHg. In this paper, we define a relaxed version of this criteria by loosening the threshold by 10mmHg, i.e., IDH-Risk, defined as SBP$<$100mmHg when predialysis SBP$<$160mmHg and SBP$<$110mmHg when predialysis SBP$\geq$160mmHg, characterizes patients that are at the risk of becoming hypotensive. As discussed later, this margin accounts for the vasoconstriction that takes place in the digital arteries to prevent hypotension. Therefore, the proposed sensor can predict the IDH events before the drop in the SBP is observed. Hence, one can avoid punishing the classifier for early detection of IDH by using the IDH-Risk criteria. This would also match the underlying physiological responses that are responsible for maintaining homeostasis (baroreflex) [7].

II. The Polyvinylidene Fluoride Ring

We are proposing a polyvinylidene fluoride (PVDF) based sensor, shown in Fig. 1, in the form of a ring that can measure the movements of the arterial wall as pulse passes through the digital arteries. The mechanical movements are transformed into a voltage that can be measured by an acquisition device. The device will raise an alarm as soon as the patterns in the signal indicate that IDH is likely to happen. The sensor, combined with the analytics to process the acquired signal,

[1]Sardar Ansari is with the Department of Emergency Medicine, University of Michigan, Ann Arbor, MI, 48109 USA. e-mail: sardara@med.umich.edu.

[2]Negar Farzaneh is with the Department of Computational Medicine and Bioinformatics, University of Michigan, Ann Arbor, MI, 48109 USA. e-mail: negarf@umich.edu.

[3]Michael Heung is with the Department of Internal Medicine, University of Michigan, Ann Arbor, MI, 48109 USA. e-mail: mheung@med.umich.edu.

[4]Kenn Oldham is with the Department of Mechanical Engineering, University of Michigan, Ann Arbor, MI, 48109 USA. e-mail: oldham@umich.edu.

[5]Harm Derksen is with the Department of Mathematics, University of Michigan, Ann Arbor, MI, 48109 USA. e-mail: hderksen@umich.edu.

[6]Kevin R. Ward is with the Department of Emergency Medicine, University of Michigan, Ann Arbor, MI, 48109 USA. e-mail: keward@med.umich.edu.

[7]Kayvan Najarian is with the Department of Computational Medicine and Bioinformatics, the Department of Emergency Medicine and the Electrical Engineering and Computer Science Department, University of Michigan, Ann Arbor, MI, 48109 USA. e-mail: kayvan@med.umich.edu.

*The author is a member of the Michigan Center for Integrative Research in Clinical Care (MCIRCC), University of Michigan, Ann Arbor, MI, 48109 USA.

978-1-5090-2455-1/16/$31.00 ©2016 IEEE

Fig. 1. The wireless version of the ring and the acquisition armband.

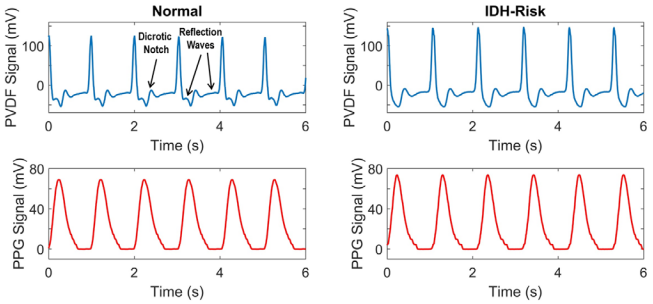

Fig. 2. On the left, the PVDF and PPG signals from a Normal section are shown. On the right, the PVDF and PPG signals for the same subject from an IDH-Risk section (before the SBP drops) are shown. The change in the pattern of the PVDF signal is evident while the morphology of the PPG signal remains the same.

provides a tool for non-invasive continuous monitoring of vascular tone.

An example of the collected PVDF and PPG signals during Normal and IDH-Risk periods are shown in Fig. 2. The PVDF signal not only shows the heart beat and the Dicrotic notch, it also exhibits the reflection waves which cannot be extracted from the PPG signal. The reflection waves diminish during IDH as a result of vasoconstriction which is one of the mechanisms that human body uses to prevent hypotension [8]. This happens before the change in the SBP becomes apparent. As a result, the morphology of the PVDF signal can be used to predict the incidence of IDH. On the other hand, the morphology of the PPG signal does not exhibit any changes.

III. Data Collection

The PVDF signal along with photoplethysmography (PPG), electrocardiogram (ECG) and accelerometer signals were collected from patients undergoing dialysis at the in-patient acute dialysis unit at University of Michigan. A total of nine subjects participated in the study, including six female and three male subjects, two of which experienced IDH. A third subject was hypotensive before and throughout the dialysis session due to septic shock. This subject was labeled as negative since the underlying mechanisms that

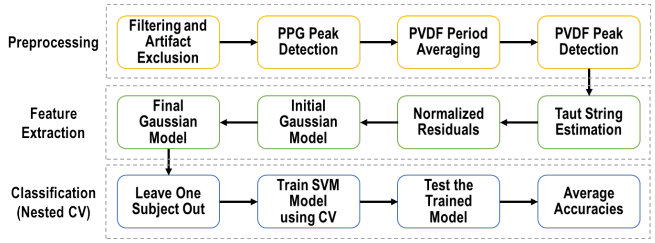

Fig. 3. The signal analysis is composed of preprocessing, feature extraction and classification, each comprised of several steps.

cause hypotension in septic shock are different from IDH in nature. In fact, septic shock is caused by gross vasodilation, due to a phenomenon called Cytokine Storm, which leads to lower BP levels [9]. The aim of this work is to create a classifier that only detects hypotension when it is caused during dialysis as a result of fluid removal from the intravascular space.

The ring was placed on the hand opposite to the arm that was used as the dialysis access, except for one subject whose non-access arm was broken. The signals were collected using a Biopac MP150 module along with BN-PPGED and BN-RSPEC to acquire the PPG and ECG signals. The PVDF sensor was connected to a DA100C module that filtered and amplified the signal. The cut-off frequency for the low-pass filter was 10Hz and the amplification gain was 50. The signals were stored on a laptop and analyzed retrospectively.

IV. Signal Analysis

The collected signals were analyzed using MATLAB software running on a 64-bits PC with a 3.4GHz Intel Xeon processor and 32GBs of memory. After preprocessing, the extracted features from the signals were used to classify the Normal and IDH-Risk sections of the signals. Different steps of data analysis are shown in Fig. 3 and each step is further explained in the following sections.

A. Preprocessing

In this work, the morphology of the PVDF signal is investigated to detect incidents of IDH while the PPG signal is used as a reference to extract the heart beats since the PPG signal is less susceptible to motion artifacts. As the first step, the regions of the data where both PPG and PVDF signals are corrupted were detected and removed from the original signals manually since motion artifact reduction is not within the scope of this paper. This step should be later replaced by a motion artifact reduction algorithm. Then, the peaks of the PPG signal are detected and used to separate each period of the PVDF signal. To detect the peaks in the PPG signal, a 10 seconds long sliding window was used and MATLAB's *findpeaks* function was applied to each window. Two detection criteria were used for peak detection. First, the minimum distance between two consecutive peaks should be at least 200 milliseconds (max heart rate of 300 beats per minute). Second, the amplitude of a peak needs to be higher than that window's 75^{th} percentile. Then, the PPG peaks are used to remove the artifacts from the PVDF signals. Each

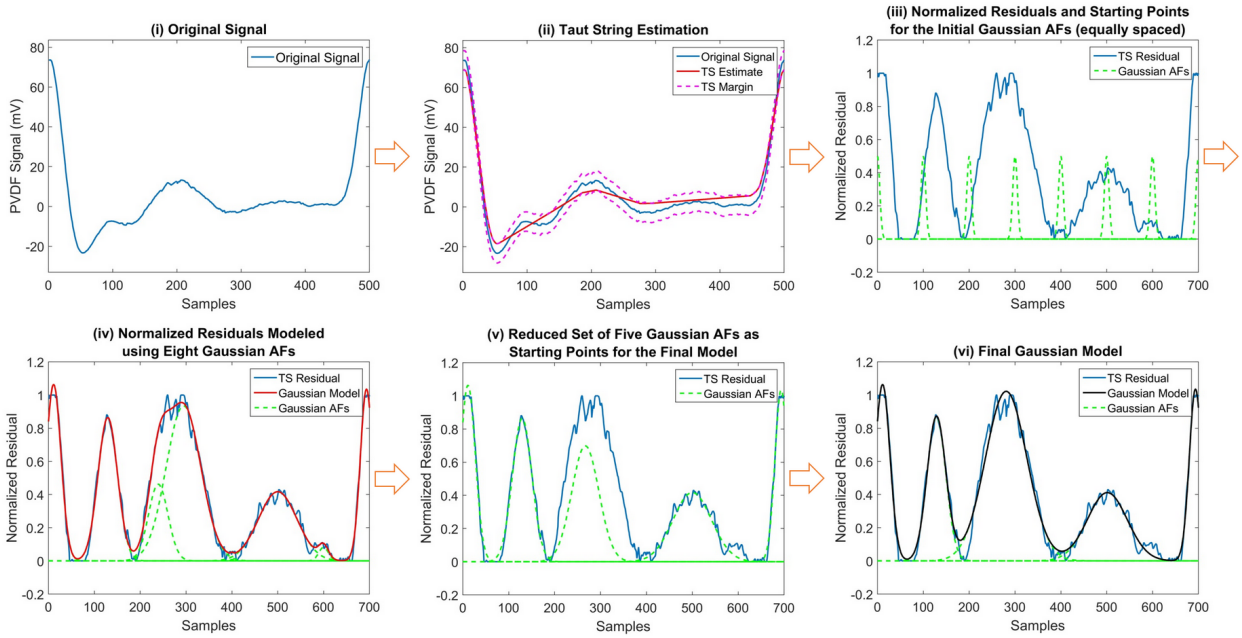

Fig. 4. The feature extraction steps are shown. (i) shows the original signal whose taus string estimate is shown in (ii). The estimation residuals after normalization between 0 and 1 are shown in (iii) along with the eight equally spaced Gaussian AFs that are used to model residuals. The Gaussian estimate and the constituting Gaussian AFs are depicted in (iv), which are combined to form the five Gaussian AFs in (v) used for initialization of the final model. The final model and its constituting Gaussian AFs are shown in (vi).

period of the PVDF signal is substituted by a *clean* version of that period by averaging 30 periods before and after that period including the period itself. The averaging is done by interpolating all the periods to have 500 samples and stacking them on top of each other. The clean period is found by finding the median of each sample across the 61 periods and interpolating the results back to the original size of the period. This step will eliminate the noise and motion artifacts from the PVDF signal.

Finally, the peaks in the PVDF signal are found using the clean signal. Let us denote the i^{th} peak in the PPG signal by p_i^{PPG}. The $(i+1)^{\text{th}}$ peak in the PVDF signal, p_i^{PVDF} can be found by finding the index of the maximum value from $p_i^{\text{PVDF}} + 10$ms to p_{i+1}^{PPG} given that the PPG signal is delayed compared to the PVDF signal.

B. Feature Extraction

The PVDF peaks are used to extract features from the periods of the PVDF signal. One period of the signal (between two consecutive peaks) is selected every 60 seconds and interpolated to 700 samples and used for feature extraction. A piece-wise linear estimation algorithm called taut string is used to estimate the general outline of the period [10], [11]. The taut string algorithm finds a piece-wise linear estimation by minimizing the total length of the line pieces such that the estimation error at any given point is less than a parameter ε. In this work, the ε value is selected to be equal to 5% of the amplitude of the period (Maximum$-$Minimum). The estimation residuals represent the small peaks including the reflection waves. The residual signal is modeled using Gaussian activation functions (AF) after being normalized between zero and one. Eight Gaussian AFs are equally spaced to model the 700 samples in the period using the nonlinear least squares method and Levenberg-Marquardt algorithm. The number of AFs is chosen experimentally as the lowest number of Gaussian AFs that can model all the peaks of interest. The initial values for the Gaussian AF amplitude and spread are 0.5 and 5, respectively. After finding the best match, five Gaussian AFs are selected from the eight that are used for modeling. This is done by combining the AFs whose means are closer than 75 samples. The two AFs are combined by averaging their mean, standard deviation and amplitude. If there are more than five Gaussian AFs remaining after this step, the five AFs with the highest amplitudes are selected. Next, the parameters for these five AFs are used to initialize a Gaussian model with five Gaussian AFs to model the period. After minimizing the squared errors, the parameters of these five Gaussian AFs are used as features for machine learning. This leads to a classification problem with 15 input variables and two classes.

C. Classification

The feature extraction produces 1590 instances from nine subjects including a total of 237 positive (IDH-Risk) instances from two subjects that experienced IDH. Each instance consists of 15 values. The negative class is defined as instances with normal SBP values and the positive class is defined as instances with a high risk of IDH (SBP$<$100mmHg when pre-dialysis SBP$<$160mmHg and SBP$<$110mmHg when pre-dialysis SBP$\geq$160mmHg). A double cross-validation (CV) approach is used to train support vector machines (SVM) to classify the Normal and IDH-

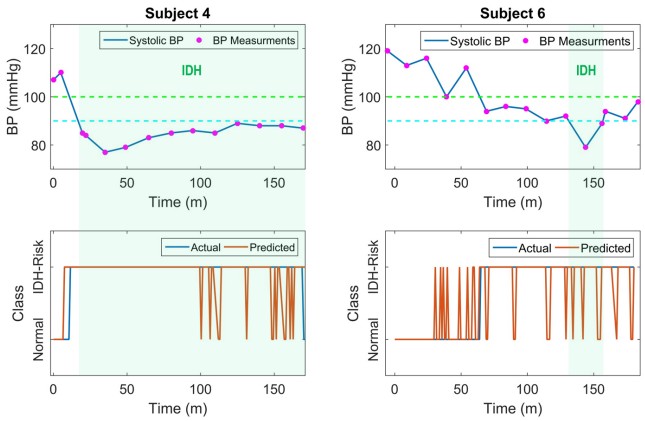

Fig. 5. The two subjects that experienced IDH are depicted in this figure. The green zones indicate the IDH episodes (SBP<90mmHg). The top figures show the SBP and the purple dots indicate the BP measurements by the BP cuff. The two limits indicate the IDH threshold (90mmHg) and the IDH-Risk threshold (100mmHg). The bottom plots show the actual classes as well as the predicated classes by the SVM model which was trained using the dataset that excluded the corresponding subject during nested CV.

Risk instances. In the outer fold, one of the nine subjects is left aside for testing. Then, a regular CV (non-subject wise) is performed in the inner fold to find the best SVM model after the data is standardized. Linear and Gaussian kernels are used in the training phase. Eleven values ranging from 0.01 to 1000 are used for the SVM's cost parameter and 11 values from 0.01 to 100 are used for Gaussian kernel's σ parameter. Also, the misclassification costs are set to compensate for the class size imbalance with the IDH-Risk class weighted higher than the Normal class with a ratio of the Normal class size divided by IDH-Risk class size. The best model in the inner fold is selected and tested using the test subject from the outer fold. The accuracies from the test subjects are averaged across the outer folds to find the overall accuracy of the method.

V. Results

The nested CV approach explained in the previous section leads to a detection sensitivity and specificity of 87.76% and 88.25%, respectively, and an overall accuracy of 88.17%$\pm$10.19% for the instances. For the negative subjects, who did not experience IDH, the average accuracy is 89.08% while the instances belonging to the positive subjects (subjects 4 and 6) were correctly classified 84.54% of times. The SBP values and the classification results for the two positive subjects are shown in Fig. 5. Subject 4 experiences IDH about 17 minutes after the beginning of dialysis while the actual BP measurement that revealed the incidence of IDH was made about 3 minutes later. The trained SVM model for this subject (using nested CV) shows the first indication for IDH about 9 minutes into the dialysis session and shows a consistent pattern for most of the session. As a result, the proposed ring would have allowed the practitioners to predict IDH 11 minutes in advance. For subject 6, the patient does not experience IDH until 131 minutes into the session. However, the SVM model shows the first signs of the change in the morphology of the PVDF signal 100 minutes earlier. The pattern becomes consistent around 68 minutes into the dialysis was started when the SVM model indicates an IDH-Risk for five consecutive minutes. This conservative criteria for detection of IDH would have resulted in predicting that the patient will become hypotensive 63 minutes before the patient experienced IDH and 76 minutes prior to the BP measurement that indicated the incidence of IDH.

VI. Conclusions

The proposed ring and analytics was shown to be effective in predicting the IDH. It can be used for non-invasive and continuous monitoring of patients in the dialysis unit given the ease of use and the low cost of making the ring. However, the system needs to be further validated using a larger dataset with more positive cases. Moreover, the application of the proposed ring in other areas where the changes in vascular tone are of interest, such as hypovolemia, heart failure, hypertension and stress, should be investigated.

References

[1] March 2015 report to the congress: Medicare payment policy, chapter 6. [Online]. Available: http://www.medpac.gov/documents/reports/chapter-6-outpatient-dialysis-services-(march-2015-report).pdf?sfvrsn=0

[2] B. F. Palmer and W. L. Henrich, "Recent advances in the prevention and management of intradialytic hypotension," *Journal of the American Society of Nephrology*, vol. 19, no. 1, pp. 8–11, 2008.

[3] B. V. Stefánsson, S. M. Brunelli, C. Cabrera, D. Rosenbaum, E. Anum, K. Ramakrishnan, D. E. Jensen, and N.-O. Stålhammar, "Intradialytic hypotension and risk of cardiovascular disease," *Clinical Journal of the American Society of Nephrology*, vol. 9, no. 12, pp. 2124–2132, 2014.

[4] J. E. Flythe, H. Xue, K. E. Lynch, G. C. Curhan, and S. M. Brunelli, "Association of mortality risk with various definitions of intradialytic hypotension," *Journal of the American Society of Nephrology*, vol. 26, no. 3, pp. 724–734, 2015.

[5] T. Shoji, Y. Tsubakihara, M. Fujii, and E. Imai, "Hemodialysis-associated hypotension as an independent risk factor for two-year mortality in hemodialysis patients," *Kidney international*, vol. 66, no. 3, pp. 1212–1220, 2004.

[6] HCUP National Inpatient Sample (NIS), Healthcare Cost and Utilization Project (HCUP), Agency for Healthcare Research and Quality, Rockville, MD, 2013. [Online]. Available: www.hcup-us.ahrq.gov/nisoverview.jsp

[7] B. H. McGhee and E. J. Bridges, "Monitoring arterial blood pressure: what you may not know," *Critical Care Nurse*, vol. 22, no. 2, pp. 60–79, 2002.

[8] D. Baim and W. Grossman, *Cardiac catheterization, angiography, and intervention*. Williams & Wilkins, 1996. [Online]. Available: https://books.google.com/books?id=wmhsAAAAMAAJ

[9] R. Cecil, L. Goldman, J. Bennett, and J. Drazen, *Cecil Textbook of Medicine*, ser. Cecil Textbook of Medicine. W.B. Saunders, 2000. [Online]. Available: https://books.google.com/books?id=LE5GPgAACAAJ

[10] R. Barlow, H. Brunk, D. Bartholomew, J. Bremner, and M. U. C. D. O. STATISTICS., *Statistical Inference Under Order Restrictions: The Theory and Application of Isotonic Regression*, ser. Wiley Series in Probability and Mathematical Statistics. Defense Technical Information Center, 1972. [Online]. Available: https://books.google.com/books?id=cE-0AQAACAAJ

[11] P. Davies and A. Kovac, "Local extremes, runs, strings and multiresolution," *Annals of Statistics*, pp. 1–48, 2001.